Supplementary material

Optimisation of NMR dynamic models II. A new methodology for the dual optimisation of the model-free parameters and the Brownian rotational diffusion tensor.

by Edward J. d'Auvergne and Paul R. Gooley

List of Figures

S1 The Brownian rotational diffusion tensor of OMP S4
S2 OMP internal dynamics comparison S5
S3 OMP correlation time differences S6

List of Tables

S1 Replication and extension of Schurr's Table 4 . . . . . S2
S2 Summary of the new model-free optimisation protocol applied to Schurr's Table 4 data S3
S3 OMP NMR structure 1JYT and the new model-free optimisation protocol S3
S4 OMP X-ray structure 1F35 and the new model-free optimisation protocol S3
S5 OMP model-free parameter values S7
S5 OMP model-free parameter values S8
S5 OMP model-free parameter values S9

Table S1: Replication and extension of Schurr's Table 4[a] where R_1, R_2, and NOE data at both 500 MHz and 600 MHz were generated for vectors at certain angles ϵ from the major axis of the spheroid, with $\tau_m = 8.5$ ns, $\mathfrak{D}_{ratio} = 1.3$, and true model-free model $m2$ parameter values of $S^2 = 0.80$ and $\tau_e = 50$ ps.

	Angle from the major axis of the spheroid – ϵ											
	0.0°	18.2°	31.8°	41.4°	49.5°	56.6°	63.3°	69.5°	75.5°	81.4°	87.1°	90.0°
Model $m5$[b,c]												
S^2	0.803	0.804	0.803	0.802	0.801	0.791	0.778	0.768	0.761	0.756	0.754	0.754
S_f^2	1.0	1.0	1.0	1.0	1.0	0.853	0.852	0.852	0.852	0.852	0.852	0.852
τ_s (ps)	37.7	40.0	43.9	47.2	49.9	440.3	689.2	829.3	920.6	977.3	1004.5	1007.9
$\chi^2(\hat{\theta})$[d]	44.50	30.73	12.25	3.03	0.06	0.57	0.92	1.13	1.29	1.39	1.44	1.45
Model $m4$[b,c]												
S^2	0.751	0.760	0.775	0.788	0.800	0.799	0.798	0.797	0.796	0.795	0.794	0.794
τ_s (ps)	38.6	40.2	43.4	46.6	49.8	52.0	53.7	54.9	55.8	56.4	56.7	56.7
R_{ex}	1.21	1.00	0.63	0.31	0.04	0.0	0.0	0.0	0.0	0.0	0.0	0.0
$\chi^2(\hat{\theta})$[d]	2.64	1.86	0.77	0.20	0.00	1.03	4.16	8.07	11.77	14.60	16.12	16.31
AIC model selection[c] (sphere)												
Model[b]	$m4$	$m4$	$m4$	$m4$	$m2$	$m2$	$m5$	$m5$	$m5$	$m5$	$m5$	$m5$
S^2	0.751	0.760	0.775	0.788	0.801	0.799	0.778	0.768	0.761	0.756	0.754	0.754
S_f^2	1	1	1	1	1	1	0.852	0.852	0.852	0.852	0.852	0.852
τ_e or τ_s (ps)	38.6	40.2	43.4	46.6	49.9	52.0	689.2	829.3	920.6	977.3	1004.5	1007.9
R_{ex} (s^{-1})	1.21	1.00	0.63	0.31	0	0	0	0	0	0	0	0
$\chi^2(\hat{\theta})$[d]	2.64	1.86	0.77	0.20	0.06	1.03	0.92	1.13	1.29	1.39	1.44	1.45
AIC model selection for model MI (local τ_m)												
Model[b]	$tm2$	$tm2$	$tm2$	$tm2$	$tm2$	$tm2$	$tm2$	$tm2$	$tm2$	$tm2$	$tm2$	$tm2$
S^2	0.800	0.800	0.800	0.801	0.801	0.801	0.801	0.801	0.801	0.801	0.801	0.801
τ_e or τ_s (ps)	50.0	50.1	50.2	50.2	50.3	50.4	50.4	50.5	50.5	50.5	50.5	50.5
local τ_m (ns)	9.35	9.22	8.99	8.80	8.63	8.49	8.38	8.29	8.23	8.19	8.17	8.17
$\chi^2(\hat{\theta})$[d]	$4e^{-28}$	$6e^{-6}$	$5e^{-5}$	$1e^{-4}$	$2e^{-4}$	$3e^{-4}$	$4e^{-4}$	$5e^{-4}$	$5e^{-4}$	$6e^{-4}$	$6e^{-4}$	$6e^{-4}$
Final global model MIII[e] ($\chi^2 = 2.782e^{-27}$)												
Model[b]	$m2$	$m2$	$m2$	$m2$	$m2$	$m2$	$m2$	$m2$	$m2$	$m2$	$m2$	$m2$
S^2	0.8	0.8	0.8	0.8	0.8	0.8	0.8	0.8	0.8	0.8	0.8	0.8
τ_e (ps)	50	50	50	50	50	50	50	50	50	50	50	50

[a] from Schurr et al., (1994).

[b] The standard model-free models are defined in 1.0–1.9 of Paper I and the model-free models with a local τ_m parameter, $tm0$ to $tm9$, are defined in the same paper.

[c] Individual residues were optimised separately. Spherical diffusion was assumed with τ_m fixed at 8.6 ns during minimisation.

[d] $\hat{\theta}$ is the parameter vector at the minimum. These χ^2 values cannot be directly compared to those in Schurr94 et al., (1994) as their definitions are different.

[e] The final global model is the prolate spheroid, the true model underlying the relaxation data. The new model-free optimisation protocol was employed and the prolate spheroid was selected by AIC model selection between models MI to MV. This final model is identical to the true model underlying the relaxation data to within machine precision.

Table S2: Summary of the new model-free optimisation protocol applied to Schurr's data from Table 4[a] where the true model underlying the relaxation data is a prolate spheroid with $\tau_m = 8.5$ ns and $\mathfrak{D}_{ratio} = 1.3$.

Global model	Convergence[b] i	Parameter number[c] k	$\chi^2(\hat{\theta})$[d]	AIC[e] $\left(\chi^2(\hat{\theta}) + 2k\right)$
MI (local τ_m)	2	36	0.00374	72.00374
MII (sphere)	2	35	14.00102	84.00102
MIII (prolate spheroid)	2	28	0.00000	56.00000
MIV (oblate spheroid)	2	28	0.00388	56.00388
MV (ellipsoid)	2	30	0.00000	60.00000

[a] from Schurr et al., 1994.
[b] i is the number of iterations of the new protocol required for convergence which, in this case, is defined as a change of χ^2 of less than $1e^{-25}$. The minimum number of iterations required to be able to test convergence is 2. i does not include the initial stage whereby the local τ_m parameters are stripped from the global model MI, the model-free parameters are held fixed, then the diffusion tensor is minimised.
[c] k is the total number of parameters in the global model. It is the sum of the number of diffusion parameters added to the sum of all model-free parameters for all residues.
[d] $\hat{\theta}$ is the parameter vector at the minimum which includes all diffusion and model-free parameters.
[e] The model which best fits the relaxation data is that with the lowest criterion value (d'Auvergne and Gooley, 2003).

Table S3: Summary of the new model-free optimisation protocol for the OMP NMR structure 1JYT.

Global model	Parameter number	$\chi^2(\hat{\theta})$	AIC
MI (local τ_m)	379	191.711	949.711
MII (sphere)	305	269.722	879.722
MIII (prolate spheroid)	300	252.652	852.652
MIV (oblate spheroid)	304	261.191	869.191
MV (ellipsoid)	301	247.873	849.873

Table S4: Summary of the new model-free optimisation protocol for the OMP X-ray crystallographic structure 1F35.

Global model	Parameter number	$\chi^2(\hat{\theta})$	AIC
MI (local τ_m)	379	191.711	949.711
MII (sphere)	305	269.722	879.722
MIII (prolate spheroid)	294	252.819	840.819
MIV (oblate spheroid)	303	258.903	864.903
MV (ellipsoid)	300	241.318	841.318

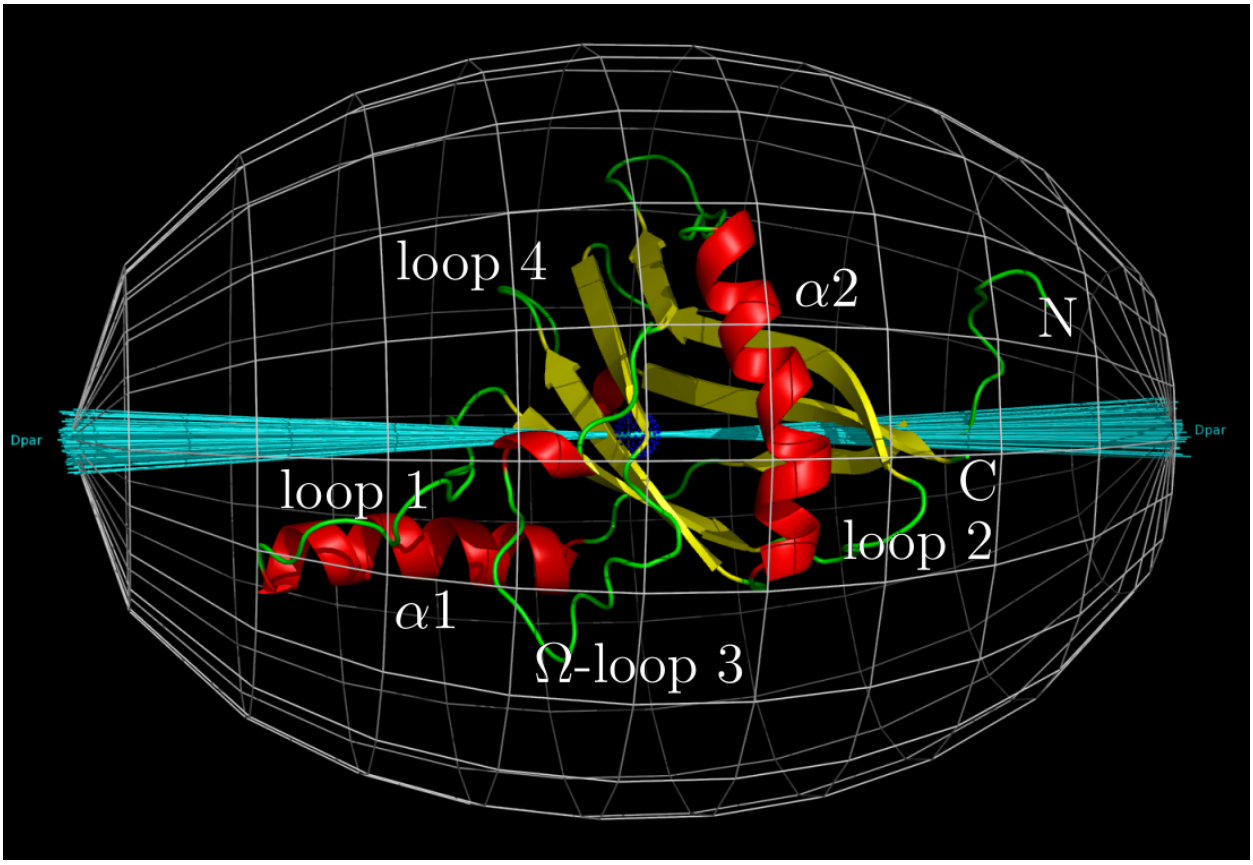

Figure S1: The Brownian rotational diffusion tensor of OMP as determined by the new model-free optimisation protocol. The tensor is the prolate spheroid using the 1F35 X-ray structure. Blue lines correspond to the $\mathfrak{D}_{\parallel}$ axes of 200 Monte Carlo simulations. The tensor geometric object is positioned at the centre of mass and scaled such that the rotational diffusion rate per Angstrom is 5.56e5 $s^{-1}Å^{-1}$. The diffusion tensor object was created as a PDB file by relax and displayed by relax through PyMOL (DeLano, 2002).

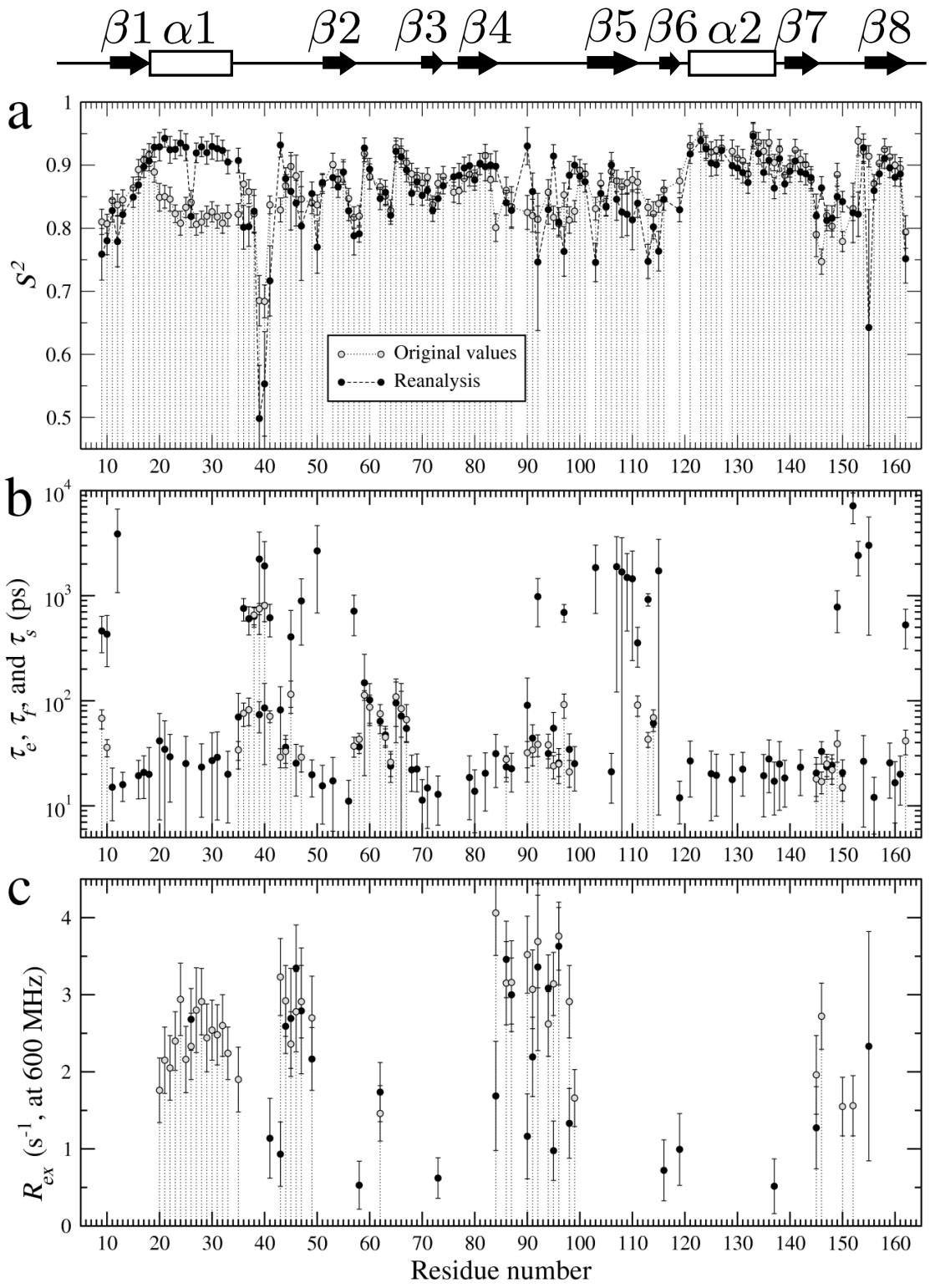

Figure S2: OMP internal dynamics comparison between the original analysis (grey circles) and the reanalysis using the new model-free optimisation protocol and the program relax (black circles). The model-free parameters compared include (a) the generalised order parameter S^2, (b) all effective correlations times τ_e, τ_f, and τ_s, and (c) the chemical exchange parameter R_{ex}. These Grace plots were created by relax.

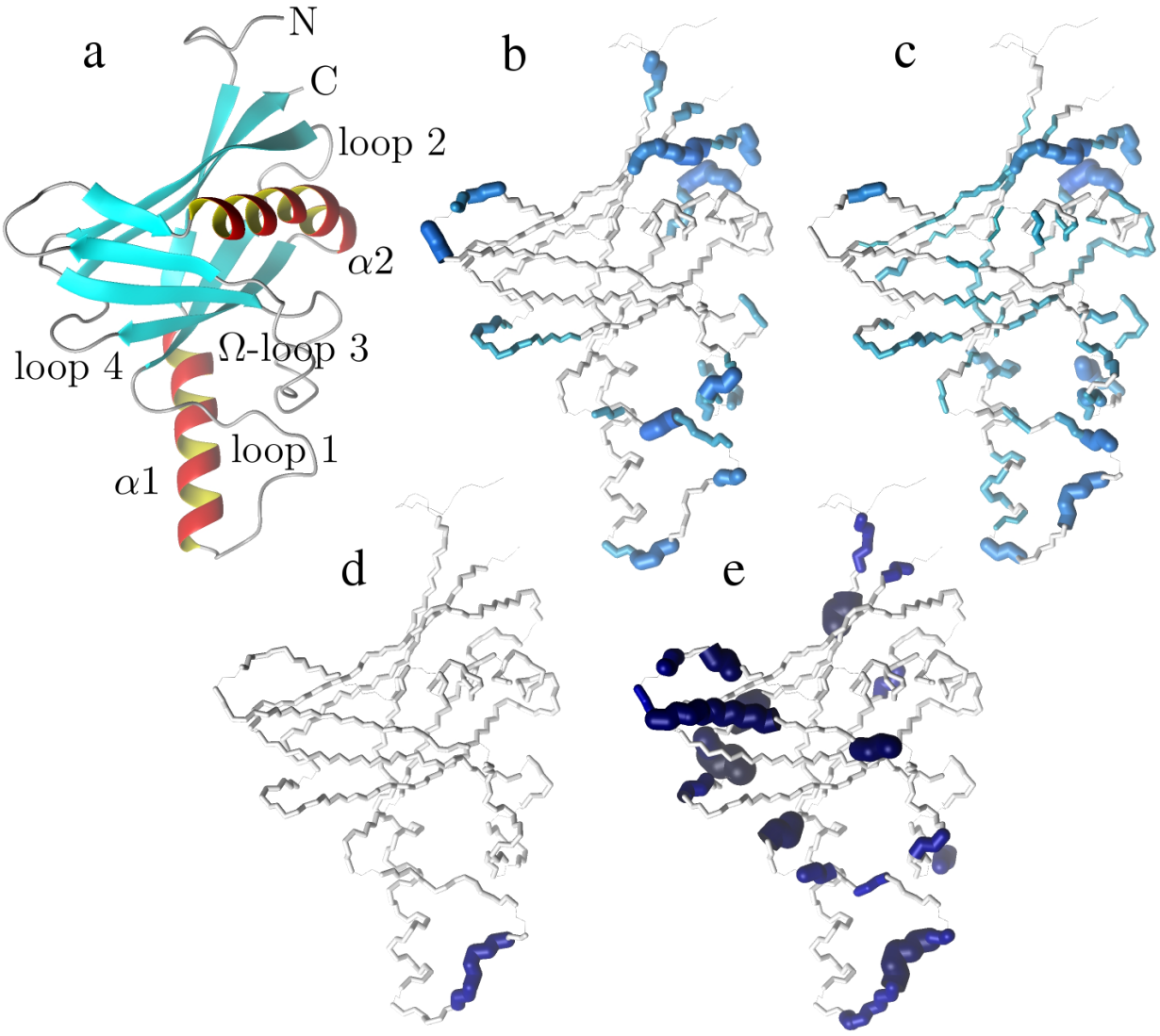

Figure S3: Illustrations of the OMP X-ray crystallographic structure (1F35) demonstrating the correlation time differences between the results of the original model-free analysis and those of the reanalysis. The reference orientation of the structure (a) is shown as a Molmol ribbon diagram. The fast correlation time parameters, defined as values less than 200 ps, are mapped onto the structure for (b) the original results verses (c) the new results. The slow correlation times, defined as values greater than 200 ps, are mapped onto the structure for (d) the original and (e) new analysis. Both the colour and bond width reflect the timescale of the motion – the thicker the bond the slower the motion. White bonds indicate residues whereby no internal correlation times could be statistically extracted from the relaxation data. Bonds drawn as thin black lines represent residues for which no data was available. To accurately pinpoint the position of the motions, backbone bonds between C_α atoms are coloured rather than the bonds of the residue to which the NH vector belongs. The Molmol images were generated by macros created by relax.

Table S5: OMP model-free parameter values for the prolate spheroid using the 1F35 X-ray structure, as determined by the new model-free optimisation protocol.

Residue	Model	S^2	S_f^2	$\tau_e < 100$ or τ_f (ps)	$\tau_e > 100$ or τ_s (ps)	R_{ex} (600.0 MHz) (s^{-1})
Gln9	$m5$	0.759±0.041	0.868±0.033		461.63±175.28	
Gln10	$m5$	0.780±0.022	0.843±0.038		429.60±218.32	
Leu11	$m2$	0.828±0.018		15.05±7.86		
Asp12	$m5$	0.779±0.040	0.817±0.020		3869.35±2799.65	
Met13	$m2$	0.822±0.014		15.92±4.94		
Leu15	$m1$	0.849±0.016				
Val16	$m2$	0.869±0.013		19.37±7.72		
Leu17	$m2$	0.897±0.017		20.83±9.11		
Asp18	$m2$	0.907±0.016		19.96±15.88		
Gln19	$m1$	0.928±0.016				
Asp20	$m2$	0.929±0.023		41.54±34.19		
Leu21	$m2$	0.943±0.014		34.54±29.72		
Thr22	$m2$	0.924±0.021		29.30±18.46		
Lys23	$m1$	0.925±0.015				
Gln24	$m1$	0.935±0.020				
Met25	$m2$	0.928±0.021		25.28±20.58		
Arg26	$m3$	0.819±0.017				2.680±0.402
Leu27	$m1$	0.919±0.016				
Arg28	$m2$	0.929±0.016		23.36±15.58		
Val29	$m1$	0.920±0.018				
Glu30	$m2$	0.930±0.020		26.93±22.76		
Ser31	$m2$	0.926±0.020		28.96±21.64		
Leu32	$m1$	0.923±0.016				
Lys33	$m2$	0.905±0.019		19.98±13.10		
Arg35	$m2$	0.907±0.020		70.04±47.59		
Gly36	$m5$	0.802±0.035	0.903±0.027		757.45±183.78	
Glu37	$m5$	0.803±0.031	0.913±0.022		603.21±180.39	
Lys38	$m2$	0.827±0.035			634.71±132.74	
Lys39	$m6$	0.498±0.084	0.733±0.055	73.70±24.18	2228.30±1800.96	
Gln40	$m6$	0.553±0.083	0.810±0.064	85.51±60.82	1918.09±1352.08	
Asp41	$m7$	0.717±0.056	0.839±0.036		615.95±211.29	1.138±0.518
Glu43	$m4$	0.932±0.019		81.88±54.13		0.931±0.418
Lys44	$m4$	0.879±0.017		36.14±10.77		2.590±0.352
Leu45	$m7$	0.859±0.061	0.935±0.047		405.28±318.75	2.692±0.649
Leu46	$m4$	0.840±0.036		25.45±13.07		3.345±0.560
Arg47	$m7$	0.803±0.086	0.870±0.059		891.37±552.96	2.791±0.816
Ala49	$m4$	0.855±0.019		19.76±7.62		2.166±0.407
Glu50	$m5$	0.770±0.041	0.839±0.026		2669.67±1983.77	
Ser51	$m2$	0.872±0.014		15.50±8.79		
Tyr53	$m2$	0.880±0.016		17.31±11.58		
Arg54	$m1$	0.866±0.017				
Leu55	$m1$	0.889±0.020				
Asp56	$m2$	0.827±0.016		11.09±6.38		
Glu57	$m5$	0.788±0.030	0.865±0.040		712.75±296.99	
Ile58	$m4$	0.791±0.013		36.45±4.98		0.529±0.312
Gln59	$m2$	0.927±0.016			148.09±128.73	
Gln60	$m2$	0.894±0.017			101.88±43.78	
Lys62	$m4$	0.847±0.018		63.80±15.32		1.737±0.383
Leu63	$m2$	0.857±0.019		47.24±9.82		

Table S5: OMP model-free parameter values for the prolate spheroid using the 1F35 X-ray structure, as determined by the new model-free optimisation protocol.

Residue	Model	S^2	S_f^2	$\tau_e < 100$ or τ_f (ps)	$\tau_e > 100$ or τ_s (ps)	R_{ex} (600.0 MHz) (s^{-1})
Gln64	$m2$	0.821±0.014		23.90±7.19		
Phe65	$m2$	0.922±0.017		95.35±55.53		
Asp66	$m2$	0.913±0.017		71.61±74.24		
His67	$m2$	0.892±0.019		54.54±13.70		
Trp68	$m2$	0.855±0.017		22.05±8.34		
Asp69	$m2$	0.873±0.015		22.39±8.80		
Val70	$m2$	0.852±0.016		11.32±6.48		
Val71	$m2$	0.860±0.015		14.82±8.73		
Leu72	$m1$	0.828±0.018				
Asp73	$m4$	0.847±0.017		12.88±6.35		0.622±0.263
Lys74	$m1$	0.867±0.013				
Gly76	$m1$	0.882±0.014				
Lys77	$m1$	0.884±0.019				
Val78	$m1$	0.895±0.017				
Thr79	$m2$	0.899±0.017		18.63±11.26		
Ile80	$m2$	0.876±0.016		13.77±8.22		
Thr81	$m1$	0.902±0.017				
Gly82	$m2$	0.898±0.022		20.44±11.51		
Thr83	$m1$	0.900±0.018				
Ser84	$m4$	0.898±0.024		31.37±16.46		1.687±0.709
Asn86	$m4$	0.840±0.020		23.45±6.54		3.459±0.496
Trp87	$m4$	0.828±0.028		22.59±9.05		2.999±0.477
Asp90	$m4$	0.930±0.030		90.59±73.75		1.163±0.552
Leu91	$m4$	0.858±0.030		44.00±14.96		2.193±0.514
Thr92	$m7$	0.746±0.109	0.855±0.077		980.63±473.92	3.360±1.086
Leu94	$m4$	0.830±0.023		31.44±8.59		3.084±0.433
Met95	$m4$	0.914±0.018		54.79±22.62		0.977±0.386
Thr96	$m4$	0.810±0.023		25.66±9.37		3.629±0.502
Arg97	$m5$	0.763±0.039	0.901±0.026		692.16±132.05	
Gln98	$m4$	0.884±0.022		34.45±13.94		1.331±0.453
Leu99	$m2$	0.900±0.014		25.23±11.37		
Leu100	$m1$	0.882±0.014				
Asp101	$m1$	0.874±0.016				
Ala103	$m5$	0.746±0.030	0.813±0.020		1850.69±1173.66	
Ala104	$m1$	0.855±0.013				
Ile105	$m1$	0.834±0.013				
Phe106	$m2$	0.900±0.020		21.11±10.51		
Trp107	$m5$	0.846±0.033	0.889±0.030		1885.34±1764.07	
Arg108	$m5$	0.826±0.040	0.883±0.027		1680.73±1877.95	
Lys109	$m5$	0.822±0.034	0.873±0.029		1487.80±1027.30	
Glu110	$m5$	0.813±0.047	0.870±0.043		1447.65±1206.88	
Asp111	$m5$	0.840±0.022	0.921±0.026		354.89±145.86	
Asp113	$m5$	0.747±0.027	0.856±0.020		919.89±124.54	
Ala114	$m2$	0.802±0.019		61.12±10.09		
Met115	$m5$	0.763±0.031	0.836±0.019		1722.20±1714.03	
Asp116	$m3$	0.846±0.017				0.722±0.396
Glu119	$m4$	0.829±0.019		11.93±5.21		0.993±0.465
Asp121	$m2$	0.918±0.015		26.71±14.59		
Leu123	$m1$	0.939±0.018				

Table S5: OMP model-free parameter values for the prolate spheroid using the 1F35 X-ray structure, as determined by the new model-free optimisation protocol.

Residue	Model	S^2	S_f^2	$\tau_e < 100$ or τ_f (ps)	$\tau_e > 100$ or τ_s (ps)	R_{ex} (600.0 MHz) (s^{-1})
Glu124	$m1$	0.926±0.018				
Phe125	$m2$	0.903±0.021		20.22±13.01		
Gly126	$m2$	0.901±0.017		19.53±11.55		
Glu127	$m1$	0.923±0.017				
Leu129	$m2$	0.899±0.016		17.76±13.05		
Ser130	$m1$	0.895±0.017				
Asp131	$m2$	0.888±0.016		22.34±9.97		
Leu132	$m1$	0.873±0.017				
Ala133	$m1$	0.946±0.020				
Lys134	$m1$	0.918±0.017				
Ile135	$m2$	0.888±0.015		19.34±11.48		
Arg136	$m2$	0.908±0.022		27.88±14.57		
Lys137	$m4$	0.864±0.017		17.13±8.96		0.516±0.355
Val138	$m2$	0.910±0.020		24.99±15.90		
Met139	$m2$	0.870±0.015		18.42±8.72		
Tyr140	$m1$	0.890±0.018				
Phe141	$m1$	0.907±0.016				
Leu142	$m2$	0.889±0.015		23.34±10.83		
Ile143	$m1$	0.886±0.018				
Thr144	$m1$	0.880±0.017				
Phe145	$m4$	0.820±0.035		20.53±8.22		1.274±0.532
Gly146	$m2$	0.864±0.018		32.90±7.93		
Glu147	$m2$	0.812±0.016		23.48±5.62		
Gly148	$m2$	0.816±0.020		24.35±6.32		
Val149	$m5$	0.850±0.033	0.906±0.029		778.50±334.31	
Glu150	$m2$	0.842±0.016		20.68±6.78		
Ala152	$m5$	0.824±0.047	0.887±0.028		7156.75±2325.03	
Asn153	$m5$	0.822±0.035	0.909±0.025		2413.59±869.97	
Leu154	$m2$	0.928±0.022		26.47±20.20		
Lys155	$m7$	0.643±0.187	0.765±0.096		3009.93±2588.84	2.332±1.487
Ala156	$m2$	0.860±0.014		12.03±6.65		
Ser157	$m1$	0.886±0.016				
Val158	$m1$	0.911±0.016				
Val159	$m2$	0.896±0.015		25.67±13.86		
Phe160	$m2$	0.881±0.014		16.60±9.74		
Asn161	$m2$	0.886±0.020		19.99±9.83		
Gln162	$m5$	0.752±0.039	0.838±0.037		527.15±215.50	